

Lars Richter

# Robotized Transcranial Magnetic Stimulation

 Springer

# Robotized Transcranial Magnetic Stimulation

Lars Richter

# Robotized Transcranial Magnetic Stimulation

 Springer

Lars Richter  
Institute for Robotics and Cognitive Systems  
University of Lübeck  
Lübeck  
Germany

ISBN 978-1-4614-7359-6                      ISBN 978-1-4614-7360-2 (eBook)

DOI 10.1007/978-1-4614-7360-2

Springer New York Heidelberg Dordrecht London

Library of Congress Control Number: 2013935774

© Springer Science+Business Media New York 2013

This work is subject to copyright. All rights are reserved by the Publisher, whether the whole or part of the material is concerned, specifically the rights of translation, reprinting, reuse of illustrations, recitation, broadcasting, reproduction on microfilms or in any other physical way, and transmission or information storage and retrieval, electronic adaptation, computer software, or by similar or dissimilar methodology now known or hereafter developed. Exempted from this legal reservation are brief excerpts in connection with reviews or scholarly analysis or material supplied specifically for the purpose of being entered and executed on a computer system, for exclusive use by the purchaser of the work. Duplication of this publication or parts thereof is permitted only under the provisions of the Copyright Law of the Publisher's location, in its current version, and permission for use must always be obtained from Springer. Permissions for use may be obtained through RightsLink at the Copyright Clearance Center. Violations are liable to prosecution under the respective Copyright Law. The use of general descriptive names, registered names, trademarks, service marks, etc. in this publication does not imply, even in the absence of a specific statement, that such names are exempt from the relevant protective laws and regulations and therefore free for general use.

While the advice and information in this book are believed to be true and accurate at the date of publication, neither the authors nor the editors nor the publisher can accept any legal responsibility for any errors or omissions that may be made. The publisher makes no warranty, express or implied, with respect to the material contained herein.

Printed on acid-free paper

Springer is part of Springer Science+Business Media ([www.springer.com](http://www.springer.com))

# Acknowledgments

I express my gratitude to my supervisors who supported me during my research: Prof. Achim Schweikard for the freedom and trust to develop the project regarding my research interests; and PD Dr. Peter Trillenberg for the insights into the neuro-psychological aspects of brain stimulation which really inspired my interest for neuroscience.

Many thanks also to Prof. Alexander Schlaefer for all the advices and support, and for acting as a Mentor.

Furthermore, I express my deepest gratitude to Cornelia Rieckhoff for all the advices and help with words and deeds. Thanks also to Jrg Paysen for the technical assistance. Both of you provide an excellent working environment.

I would like to thank my colleagues at the Institute for Robotics and Cognitive Systems for the teamwork and assistance, in particular: Ralf Bruder, Floris Ernst, Fernando Gasca, Markus Finke, Christoph Metzner, and Maximilian Heinig. Additionally, I express my gratitude to Lars Matthus for the intensive discussions and the feedback regarding the project and the support on the robot.

Thanks also to Uwe Melchert and Christian Erdmann from the Institute for Neuroradiology for all the CT and MRI images, and to Reinhard Schulz from the scientific workshop for building all the parts, adapters, and holders. I further thank Stephen Oung and Gunnar Neumann for helping me with the experiments.

Furthermore, I express my gratitude to Frau Meier, substitutional for all the volunteers who participated in our studies.

Last but not least, in particular most important, I sincerely thank my parents, Alev, my brother Leif, and Jens for the motivation, moral support, and trust during all those years.

# Contents

<b>1</b>	<b>Introduction</b>	1
1.1	Transcranial Magnetic Stimulation	1
1.1.1	Principle of TMS	1
1.1.2	Applications of TMS: Single-Pulse Versus Repetitive Stimulation	3
1.1.3	TMS Coils	4
1.1.4	Motor Evoked Potentials and Motor Threshold	6
1.2	State-of-the-Art: Neuro-Navigated TMS	8
1.2.1	Head Registration and Tracking	9
1.2.2	Coil Tracking	10
1.3	Robotized TMS: Combining Neuro-Navigation with Automation	11
1.3.1	Specialized Setup	11
1.3.2	Industrial Robot Design	13
1.4	Purpose of this Work	16
1.4.1	Structure of this Work	18
	References	19

## **Part I Systematic Analysis and Evaluation of Robotized TMS in Practice**

<b>2</b>	<b>The Importance of Robotized TMS: Stability of Induced Electric Fields</b>	27
2.1	Principle of End-to-End Accuracy	28
2.2	Realization and Data Acquisition	30
2.2.1	Head Motion Measurements	30
2.2.2	Electric Field Measurements	31
2.2.3	Typical TMS Scenarios	33
2.2.4	Error Calculation	34
2.2.5	Statistical Analysis	34
2.3	Impact of Head Motion on TMS	34
2.3.1	Head Motion	34

- 2.3.2 End-to-End Accuracy . . . . . 36
- 2.4 Consequences. . . . . 40
- 2.5 Derived Requirements for Robotized TMS . . . . . 41
- References . . . . . 42
- 3 Evaluation of Robotized TMS: The Current System in Practice . . . . . 45**
  - 3.1 Optimal Coil Orientation for TMS of the Lower Limb . . . . . 45
    - 3.1.1 Experimental Realization. . . . . 46
    - 3.1.2 Stimulation Outcomes . . . . . 49
    - 3.1.3 Relevance for TMS. . . . . 52
  - 3.2 Coil-to-Scalp/Cortex Distance . . . . . 53
    - 3.2.1 TMS Recordings . . . . . 54
    - 3.2.2 Measured Motor Thresholds and Distances . . . . . 54
    - 3.2.3 Robotized TMS for Accurate Coil Positioning . . . . . 55
  - 3.3 Practical Evaluation of Robotized TMS. . . . . 55
  - References . . . . . 57
- Part II Safe and Clinically Applicable Robotized TMS**
- 4 Robust Real-Time Robot/Camera Calibration . . . . . 63**
  - 4.1 Hand–Eye Calibration . . . . . 65
  - 4.2 Online Calibration . . . . . 67
    - 4.2.1 Basic Idea of Online Calibration . . . . . 68
    - 4.2.2 Marker Calibration . . . . . 68
    - 4.2.3 Robust Real-Time Calibration . . . . . 69
    - 4.2.4 Translational Error Estimation for Marker Calibration . . . . . 71
    - 4.2.5 Error Calculation for Online Calibration . . . . . 73
    - 4.2.6 Data Acquisition for Evaluation . . . . . 73
  - 4.3 Evaluation of Online Calibration . . . . . 77
    - 4.3.1 Accuracy of Marker Calibration . . . . . 77
    - 4.3.2 Accuracy of Online Calibration . . . . . 78
  - 4.4 Benefits for Robotized TMS . . . . . 80
  - References . . . . . 83
- 5 FT-Control. . . . . 85**
  - 5.1 Basic Principles . . . . . 86
    - 5.1.1 Sensor Calibration . . . . . 87
    - 5.1.2 Gravity Compensation and Tool Calibration . . . . . 89
    - 5.1.3 Influence of the Coil’s Supply Cable . . . . . 90
  - 5.2 Implementation of FT-Control . . . . . 90
    - 5.2.1 Setup . . . . . 91

- 5.2.2 Hand-Assisted Positioning . . . . . 91
- 5.2.3 Contact Pressure Control . . . . . 93
- 5.2.4 Data Acquisition for Evaluation of FT-Control. . . . . 95
- 5.3 Results of FT-Control . . . . . 98
  - 5.3.1 Coil Calibration and Gravity Compensation. . . . . 98
  - 5.3.2 Hand-Assisted Positioning . . . . . 99
  - 5.3.3 Latency of Contact Pressure Control. . . . . 100
- 5.4 FT-Control in the Context of Robotized TMS . . . . . 100
- References . . . . . 101
  
- 6 FTA-Sensor: Combination of Force/Torque and Acceleration . . . . . 103**
  - 6.1 The FTA Sensor. . . . . 104
    - 6.1.1 Combining Acceleration with Force–Torque . . . . . 104
    - 6.1.2 Embedded System for Real-Time Monitoring . . . . . 105
    - 6.1.3 Hardware Design: Circuit Board and Casing . . . . . 106
    - 6.1.4 Calibration of IMU to FT Sensor . . . . . 108
    - 6.1.5 Data Acquisition for Evaluation of the FTA Sensor . . . . . 110
  - 6.2 Performance of the FTA Sensor . . . . . 114
    - 6.2.1 Calibration. . . . . 114
    - 6.2.2 Gravity Compensation. . . . . 116
    - 6.2.3 Latency . . . . . 118
    - 6.2.4 Realistic Worst-Case Estimate . . . . . 118
  - 6.3 FTA Sensor for Safe Robotized TMS . . . . . 119
  - References . . . . . 120
  
- 7 Optimized FT-Control with FTA Sensor . . . . . 121**
  - 7.1 Advanced Hand-Assisted Positioning . . . . . 121
  - 7.2 Integration into the Robot Server . . . . . 124
  - 7.3 TMS Coil Calibration . . . . . 126
  - 7.4 Data Acquisition for Realistic Evaluation of Optimized FT-Control. . . . . 126
    - 7.4.1 Coil Calibration and Gravity Compensation. . . . . 127
    - 7.4.2 Precision of Optimized Hand-Assisted Positioning . . . . . 127
  - 7.5 Performance of the FTA Sensor in Operation . . . . . 129
    - 7.5.1 Coil Calibration and Gravity Compensation. . . . . 129
    - 7.5.2 Precision of Optimized Hand-Assisted Positioning . . . . . 130
  - 7.6 Optimized FT-Control for Clinical Acceptance . . . . . 131
  - References . . . . . 132
  
- 8 Direct Head Tracking. . . . . 133**
  - 8.1 Direct Versus Indirect Tracking . . . . . 133
  - 8.2 FaceAPI . . . . . 134
    - 8.2.1 The FaceAPI’s Main Principle . . . . . 134



8.2.2	Evaluation of the FaceAPI for Direct Head Tracking . . . . .	135
8.2.3	Accuracy of the FaceAPI . . . . .	135
8.3	3D Laser Scans . . . . .	135
8.3.1	Implementation of Direct Head Tracking with Laser Scans . . . . .	136
8.3.2	Data Acquisition for an Experimental Validation . . . .	141
8.3.3	First Results . . . . .	142
8.4	Head Contour Generation Based on Laser Scans . . . . .	147
8.4.1	Head Scanning and Contour Generation . . . . .	147
8.4.2	Comparison to Manual Contour Generation . . . . .	148
8.4.3	Application in Robotized TMS Studies . . . . .	148
8.5	Capability of Direct Tracking for Robotized TMS . . . . .	150
	References . . . . .	150

### **Part III Discussion and Closing Remarks**

<b>9</b>	<b>Discussion . . . . .</b>	<b>155</b>
9.1	Robust Real-Time Robot/World Calibration . . . . .	156
9.2	Hand-Assisted Positioning . . . . .	157
9.3	Contact Pressure Control . . . . .	159
9.4	FTA Sensor . . . . .	159
9.5	Direct Head Tracking . . . . .	162
9.5.1	FaceAPI . . . . .	162
9.5.2	3D Laser Scans . . . . .	163
	References . . . . .	164
<b>10</b>	<b>Closing Remarks . . . . .</b>	<b>167</b>
10.1	Conclusions . . . . .	167
10.2	Outlook and Future Work . . . . .	168
10.2.1	Fully Automated TMS . . . . .	168
10.2.2	Mapping of the Spinal Roots . . . . .	169
10.2.3	Direct Head Tracking . . . . .	170
10.2.4	Double-Coil Robotized TMS . . . . .	172
10.2.5	Robotized Interleaved TMS/fMRI . . . . .	172
	References . . . . .	175
	<b>Glossary . . . . .</b>	<b>177</b>
	<b>Companies . . . . .</b>	<b>181</b>
	<b>Curriculum Vitae . . . . .</b>	<b>183</b>

# Symbols

Throughout this work the following notation applies: Vectors are denoted with an arrow, such as  $\vec{A}$ . Uppercase letters, e.g.  $M$ , refer to matrices. Coordinate systems are expressed in bold uppercase letters, such as  $\mathbf{C}$ . Transformation matrices from a coordinate system  $\mathbf{C}$  to another coordinate system  $\mathbf{D}$  are described by  ${}^{\mathbf{C}}\mathfrak{T}_{\mathbf{D}}$ . Scalars and constant values are denoted with italic lowercase letters, e.g.  $m$ .

## Coordinate Systems

<b>FT</b>	Force-torque sensor coordinate frame
<b>IMU</b>	Coordinate system of the Inertia Measurement Unit (IMU)
<b>E</b>	Coordinate frame of the robot's end effector
<b>R</b>	The robot's base
<b>C</b>	Coordinate system of the TMS coil
<b>T</b>	The tracking system's coordinate system
<b>L</b>	Coordinate frame of the laser scanning system
<b>H</b>	The patient's head
<b>M</b>	The marker's coordinate system
<b>S<sub>3</sub></b>	Coordinate system in the robot's fourth joint (link three)
<b>S<sub>2</sub></b>	Coordinate system in the robot's third joint (link two)
<b>M<sub>ref</sub></b>	Reference Image of the marker used for direct head tracking
<b>H<sub>ref</sub></b>	Reference Image of the head used for direct head tracking
<b>C<sub>ref</sub></b>	Reference Image of the coil used for direct head tracking

## Matrices

${}^{\mathbf{A}}\mathfrak{T}_{\mathbf{B}}$	Transformation matrix from $\mathbf{A}$ to $\mathbf{B}$
${}^{\mathbf{FT}}\mathfrak{T}_{\mathbf{V}}$	Calibration matrix of the force-torque sensor to convert voltage readings from FT sensor into forces and torques
$R_x$	Rotation matrix around the x-axis

$R_y$	Rotation matrix around the y-axis
$R_z$	Rotation matrix around the z-axis

## Vectors

$\vec{F}_0$	Zero force
$\vec{F}$	Any recorded force
$\vec{F}'$	Expected force for a given spatial orientation
$\vec{F}_{\text{user}}$	Gravity compensated force
$\vec{\tilde{F}}$	Damped force vector for direct robot movement
$\vec{M}$	Any recorded torque
$\vec{M}'$	Expected torque for a given spatial orientation
$\vec{M}_{\text{user}}$	Gravity compensated torque
$\vec{\tilde{M}}$	Damped torque vector for direct robot movement
$\vec{A}$	Recorded acceleration
$\vec{A}_{\text{IMU}}$	Acceleration in the IMU coordinate frame
$\vec{A}_{\text{FT}}$	Acceleration transformed into the FT coordinate frame
$\vec{V}$	Voltage reading from the FT sensor
$\vec{s}$	Tool's centroid
$\vec{E}$	(Induced) electric field
$\vec{B}$	Magnetic field

## Scalars

$m$	Tool's mass
$f_g$	Tool's gravity force (corresponding to its mass $m$ )
$f$	Force magnitude

## Constants

$g$	Gravity acceleration, with $1 g = 9.81 \text{ m/s}^2$
-----	---

# Chapter 1

## Introduction

### 1.1 Transcranial Magnetic Stimulation

The idea of Transcranial Magnetic Stimulation (TMS) for non-invasive brain stimulation is simple but brilliant: A strong, rapidly increasing current is driven through a magnetic coil placed on the head of a subject. The generated magnetic field passes through the human skull and—due to *Electromagnetic Induction*—induces an electric current inside the cortex which can lead to local stimulation [17]. However, it took almost a century, using huge magnets around the head in the very beginning, until Anthony Barker successfully introduced TMS in 1985 [5]. At this early stage, only muscle contractions could be clearly observed when stimulating the motor cortex.

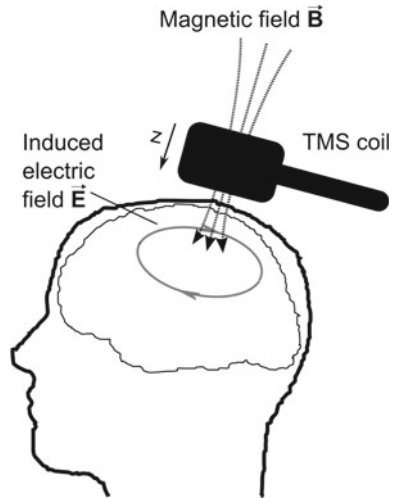
Nowadays, TMS has not only become an important tool in clinical routine, but particularly repetitive Transcranial Magnetic Stimulation (rTMS) is a promising tool for treatment of a variety of medication resistant neurological and psychological conditions.

Moreover, for (cognitive) neuroscience and brain research, TMS is a key technique to study the brain's functionality and connectivity. In general, TMS is applied for non-invasive and painless cortical brain stimulation.

#### 1.1.1 Principle of TMS

During TMS, cortical neurons are activated by a current distribution that is induced by a transient magnetic field. This time-varying magnetic field is generated by a short high-current pulse (4–20 kA) sent through a stimulation coil located on the scalp of the individual. The magnetic stimulator itself generates high voltages of 400–3,000 V. The resulting magnetic field lasts for a few milliseconds and can reach peak strengths of 1–10 T [24, 29]. This magnetic field passes easily through the human skull and induces a current density distribution that is characterized by a direction and magnitude that both vary within the cortex [71]. These quantities are determined by the coil position and geometry, and by the

**Fig. 1.1** For TMS, a rapidly changing magnetic field  $\vec{B}$  is produced by a coil and passes through the skull. This way,  $\vec{B}$  induces an electric field  $\vec{E}$  in the cortex that depolarizes neurons. In the target region, the principle component of  $\vec{B}$  can be assumed to be in  $z$ -direction



geometry and electrical conductivity of the tissue. Note that the induced current stimulates the tissues similar to electrical stimulation (Transcranial Electrical Stimulation (TES)) [66]. For TMS, the magnetic field just functions as a carrier to induce an electric current inside the cortex. Thus, TMS does not produce high currents in the skin and therefore does not result in pain. Figure 1.1 illustrates the basic principle of TMS for non-invasive brain stimulation.

For TMS, the induced electric field is perpendicular to the magnetic field and in opposite direction to the electrical current in the coil. In principle, assuming homogeneous conductivity, the induced electric field is parallel to the plane of the coil [24]. Hence, the TMS coil is tangentially placed on the head for (optimal) stimulation. However, the human brain is inhomogeneous and local conductivity differences occur. Therefore, only complex models and extensive simulations are capable to predict the real current distribution inside the tissue [55, 87].

Simulations have shown that for identical magnetic fields the magnitude of the induced current in the brain critically depends on the orientation of the coil relative to underlying gyri and sulci. In fact, the induced electric field in the tissue is maximal when perpendicular to the underlying gyrus [82]. Furthermore, it has been hypothesized that pyramidal neurons are stimulated most effectively when in alignment with the current direction [21]. Thus, both, orientation and position of the stimulation, provide information on the location of cells and structures that are influenced by TMS.

Neuronal activation will ensue if the current density at the position of a pyramidal neuron exceeds a threshold value to depolarize (or hyperpolarize) the axon membrane [72]. This will cause an *Action Potential*. Even though pyramidal axons are likely to be stimulated near bends [44], also other geometrical factors, e.g., terminals and branches, may change the neuronal excitability [67]. In principle, those axons are most likely to be activated that change their orientation in relation to the induced electric field direction [24].

The strength of the electromagnetic field decreases quasi-exponentially with increasing coil distance [7]. Therefore, the depth penetration of TMS in the tissue is limited and stimulation of deeper brain areas is not possible in practice [25]. The cortical target region is thus located approximately 10–60 mm beneath the TMS coil [79] which is due to the individual scalp-to-cortex range [36]. In contrast to other cortical regions, effects of TMS on the the Primary Motor Cortex (M1) can be directly observed or measured. Stimulation of M1 in general leads to muscle twitches of the associated muscle which can be detected by visual inspection or by Electromyography (EMG) recordings using surface electrodes. In particular, the Primary Motor Hand Area (M1-HAND) is easy to stimulate with low intensities as it is relatively large and located at the surface of the precentral cortex. For the Primary Motor Leg Area (M1-LEG), on the contrary, higher intensities are required because it is located at the medial wall of the precentral gyrus. Responses to stimulation of other brain regions are indirectly detectable as evoked neural activity with Electroencephalography (EEG) [51] or changes in blood flow with functional Magnetic Resonance Imaging (fMRI) [70], Single Photon Computed Tomography (SPECT) [10] or Positron Emission Tomography (PET) [20]. See [57] or [79] for a general overview.

### ***1.1.2 Applications of TMS: Single-Pulse Versus Repetitive Stimulation***

At the very beginning of TMS, the stimulators were only able to produce single pulses. Currently, repetitive stimulators with repetition frequencies of up to 50 Hz are available [85]. The main difference between single pulse and repetitive stimulation is that rTMS can change neuronal behavior whereas single pulse TMS leads to an immediate reaction, e.g., muscle twitching.

Hence, clinical diagnosis is the main application of single pulse TMS. A single TMS pulse is applied to the motor cortex and the corresponding muscle response is recorded. For clinical routine mainly the central motor conduction time, the motor threshold, the Motor Evoked Potential (MEP) amplitude or the silent period are of importance [74]. This way, e.g., spinal cord injuries can be diagnosed and/or investigated [39].

Another interesting and promising application for single pulse TMS is motor cortex mapping. Muscle responses are recorded for different coil positions. The representation of this muscle in the cortex can now be calculated based on the set of recordings [48]. For neurosurgery, brain tumor removal can be planned and supported by motor cortex mapping [33]. Figure 1.2 displays a motor cortex mapping for the Abductor digiti minimi (ADM) muscle before and after tumor removal. It clearly shows that tumor removal (including a safety margin) is possible without damage of the cortical control of this muscle. In this way, also the cortical plasticity due to tumor growth can be investigated [18]. In brain research, motor cortex mapping helps localizing specific brain areas and motor pathways [56].

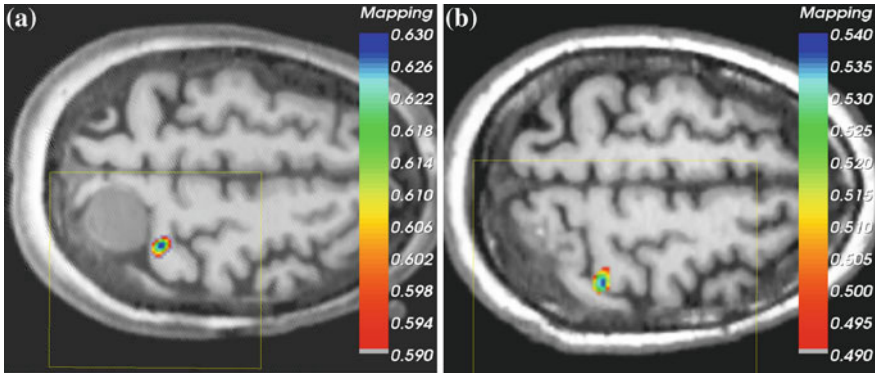


**Fig. 1.2** Brain mapping with TMS of the ADM muscle before (a) and after (b) tumor resection. Due to the tumor removal, the precentral gyrus shifted and therefore a shift in the localization of the muscle occurs. Figures from [46], with friendly permission of the author

Furthermore, single pulse TMS is also applied to produce virtual lesions to study the brain's connectivity and functionality [58, 84].

Repetitive TMS, on the contrary, can change neuronal behavior for a certain amount of time. In this case, neuronal behavior connects to the level of cortico-spinal excitability, the connectivity between the stimulated cortex and other connected brain areas, and the neuronal activity in the stimulated cortex. These effects of neuro-modulation motivate the application of rTMS in cognitive brain research and treatments of different neurological and psychiatric conditions. Depending on the stimulation frequency, rTMS is used for inhibitory or excitatory brain stimulation. Low frequency stimulation ( $< 5$  Hz) decreases and high frequency stimulation ( $> 5$  Hz) increases neuronal excitability. However, the principle and the duration of the effect are yet not fully understood. Interestingly, clinical trials have proven positive effects, e.g., for depression [19], chronic tinnitus [35] and chronic pain [49]. Typically, rTMS is applied for 15–30 min for each single treatment session.

Theta Burst Stimulation (TBS), as a novel paradigm of rTMS, is able to produce long-term effects after a relatively short period of stimulation (just a few minutes) [28]. It uses very high stimulation frequencies in small intervals with a short pause and a high number of intervals, e.g. 200 intervals with 3 pulses at 50 Hz with an interval pause of 200 ms. First studies reported positive effects, e.g., for treatment of chronic tinnitus [13, 65].

### 1.1.3 TMS Coils

For TMS mainly two coil types are available and frequently used. They vary in shape and therefore in their magnetic field properties. Circular coils (or round coils) induce a ringlike electric field below the coil's windings. This way, a large

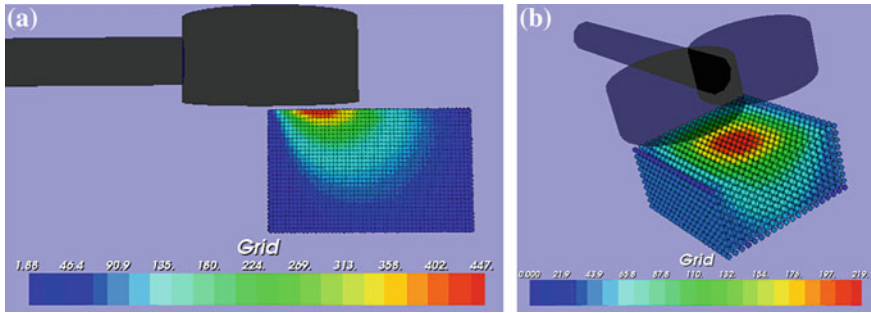


**Fig. 1.3** Electric fields of two typical TMS coils measured by a field sensor. The measures are displayed in mV as induced in the sensor. **a** The field of the circular coil is rotational symmetric. **b** The field of the figure-of-eight coil produces a focal area underneath the center. Figures from [48], with friendly permission of the author and the copyright holder, ©2008 John Wiley and Sons

cortical region is affected by the stimulation. Figure-of-eight (figure-8) or butterfly coils produce a more focal magnetic field. They consist of two circular coils that are located in parallel. Below the intersection of the two circles, the induced electrical field of both circles is added. Therefore, the induced electric field has a focus beneath the center of the intersection which is typically the center of the coil. Figure-of-eight coils are thus used for (more) focal brain stimulation. Figure 1.3 shows the spatial electric field distribution of a typical circular and a figure-of-eight coil.

Main applications of figure-of-eight coils are in rTMS experimental treatment and brain research. Circular coils are primarily used in clinical diagnosis and routine as they have a broad focus. Producing stimulation effects with these coils is thus easier than with figure-of-eight coils.

However, the magnetic field properties of both coil types are specified by the number and the diameter of the coil windings. In general, a smaller coil diameter results in a more focal electric field but has the drawback of faster coil heating. In contrast, larger coil windings lead to a better depth penetration. By increasing the number of windings also the magnetic field strength increases but at the cost of faster coil heating.

However, due to the general behavior of magnetic fields, the strength of the induced electric field decreases quasi-exponentially with depth [8, 22].

Besides these two common coil types, specialized coil designs have been introduced and investigated. The H-coil, for instance, produces a higher induced electric field compared to circular coils [68]. Therefore, it is intended for stimulation of deeper brain regions [69]. However, deeper regions cannot be targeted without stimulating superficial brain structures [16].



### 1.1.4 Motor Evoked Potentials and Motor Threshold

An easy way to detect macroscopic responses is observation of muscle contraction or twitching after motor cortex stimulation. A Motor Evoked Potential (MEP) can be measured using Electromyography (EMG) with surface electrodes over an associated muscle. The MEP represents the electrical potential at this muscle, which is a correlate of muscle contraction. In general, the stronger the muscle contraction the higher the MEP amplitude.

For the use of TMS, determination of the Motor Threshold (MT) for the target muscle is often the first step. In general, the MT is a measure of (corticomotor) excitability. It is defined as the stimulation strength at which a muscle contraction occurs with a probability of 50 %. In this case, a muscle contraction is recorded if the base-to-peak MEP amplitude exceeds 50  $\mu\text{V}$  (for the resting muscle). The MT, beside its routine application in diagnosis, plays a key role in rTMS treatments: The stimulation strength for treatment is calculated based on the individual MT [57, 79, 85]. However, the MT highly depends on the used equipment and setup, i.e., stimulator, coil and pulse waveform. The MT is therefore traditionally expressed in percentage of Maximum Stimulator Output (MSO) which makes it almost impossible to directly compare the MT between different studies. However, as the MEP amplitude has a very high variance [88], often the MT is used in brain research as a more stable quantitative measure for cortical excitability. However, also the MT can change due to vigilance, stress or muscle pretension—even within subjects [34].

As enhancement to the MT, recently the *computed electric field* on the cortex at MT strength was introduced as a more stable and comparable measure of cortical excitability. By using navigated TMS (see below) and the field properties of the TMS coil used, an estimate of the electric field strength on the cortex can be computed at MT strength which should theoretically accurately reflect the anatomy and the used system [14]. Even though first studies have shown promising results, due to the complexity of its computation, the computed electric field is far away from becoming a standard technique [31].

From a mathematical point of view, the MT is explicitly defined. However, an accurate determination is rather complex, which is mainly due to natural excitability changes [1]. Recently, different methods have been proposed to determine the MT. The three most common methods are presented in some more detail:

#### 1.1.4.1 Rossini Criterion

The first method to estimate the MT was presented in the general guidelines on TMS, published by the International Federation of Clinical Neurophysiology (IFCN) in 1994 [66]. A standardized algorithm can be derived from this method where the MT is defined as the stimulation intensity at which 5 MEPs are evoked in 10 trials [24]. After placement of the coil at the optimal stimulation site (the *hot-spot*), the

stimulation intensity is increased in steps of 5 % of MSO until MEPs larger than 50  $\mu\text{V}$  are consistently produced. Subsequently, the intensity is decreased in steps of 1 % of MSO until less than 5 MEPs larger than 50  $\mu\text{V}$  are produced in 10 trials. This intensity plus 1 is then used as the MT.

Even though this method is easy applicable and estimates the MT quite accurately, it requires a relatively high number of stimulation pulses (about 75) and is therefore relatively time-consuming [83].

#### 1.1.4.2 Two-Threshold Method

Another approach estimates an upper and a lower threshold [50]. The MT is then defined as the arithmetic mean between these two thresholds. The lower threshold is therefore defined as the highest stimulation intensity at which no positive MEP is measured in 10 consecutive stimuli. Accordingly, the upper threshold is defined as the lowest intensity at which no MEP smaller than 50  $\mu\text{V}$  is recorded in 10 consecutive stimuli.

In contrast to the Rossini methods, the two-threshold method requires about 45 stimuli to estimate the two thresholds. However, the MT is only approximated with this method.

#### 1.1.4.3 Threshold Hunting

This adaptive method is based on the assumption that the relation between the likelihood of an evoked MEP and the stimulus intensity can be modeled as a sigmoidal function. The threshold hunting method therefore calculates the probability to evoke an MEP for a given stimulus based on the already performed trials. Using a maximum likelihood estimation, based on best PEST (parameter estimation by sequential testing) [59], the most likely MT intensity is calculated [2]. For the next stimulation pulse this strength is used for measuring the MEP. It was reported that on average 17 stimulation pulses are required to calculate a reliable MT with this method [3]. As a computer is essential to use this method, Awiszus and Borckardt developed the TMS Motor Threshold Assessment Tool, a freeware program to perform this threshold hunting [4].

#### 1.1.4.4 Brief Comparison

The method by Rossini is very easy to utilize as it is straight-forward. It is therefore commonly used in clinical practice. With some experience a physician is able to reduce the number of required pulses to estimate a reliable MT. In research, the two-threshold method is at present replaced by the threshold hunting method. The advantage of this method is that it is an adaptive method that takes the previous recordings into account. Therefore, it requires a smaller number of pulses

to calculate the MT. With the available computer program, the usage is very convenient and it has become the standard method in TMS research [79]. However, as this method, and all other methods mentioned, do not take the strength of the MEP into account, it might lead to a wrong MT estimate.

## 1.2 State-of-the-Art: Neuro-Navigated TMS

Different approaches exist to locate the stimulation target and to position the coil. In its simplest way, localization is based on external anatomical landmarks, e.g., midline or ear-to-ear-line. The TMS coil is now placed in relation to these anatomical landmarks.

Commonly, a hot-spot at the M1 as the optimal stimulation site is estimated prior to actual stimulation. Therefore, different stimulation points are investigated until the best stimulation outcome, e.g. maximal muscle twitching of a specific muscle, is obtained. The hot-spot is usually estimated in the M1-HAND area. Using a *function-guided* coil positioning procedure, the stimulation site is estimated in relation to this hot-spot. Standard distances are for instance 5 cm anterior for stimulation of the Dorsolateral prefrontal cortex (DLPFC) [26], 2–3 cm anterior for stimulation of the Premotor Cortex (PMC) [23] or 3 cm posterior for the Primary Somatosensory Cortex [37].

Another way is to take advantage of the 10–20 system of electrode placement for EEG recordings [30]. The TMS coil can be placed relatively to these electrode positions [27]. With use of electrode caps, the 10–20 System is very practical. However, due to individual anatomical and functional variability, the coil positioning may lead to errors of a few centimeters—depending on the stimulation site [54].

For the proper analysis of TMS effects, exact coil positioning is essential [80]. A current technique for coil positioning and target localization is therefore the application of real-time frameless stereotaxic systems [43]. These neuro-navigation systems combine high resolution three-dimensional (3D) scans of the patient's head with a real-time tracking system [73]. Commonly, Magnetic Resonance Imaging (MRI) scans of the patient are used as navigation source. From these scans, the the three-dimensional (3D) head and the brain's anatomy are reconstructed. After registration and with tracking of TMS coil and head, the TMS coil can be positioned based on the 3D head scan. Neuro-navigated TMS has become the state-of-the-art tool for precise target localization in TMS research as it takes the individual anatomy of the patient into account [78]. Beside precise target localization, it also improves the repeatability of coil positioning within and between TMS sessions [43]. Furthermore, it was shown that neuro-navigated TMS also has its value for rTMS treatments of chronic tinnitus [40] and depression [75].

Currently, various commercial neuro-navigation TMS systems are available, e.g. Visor2<sup>TM</sup> (Advanced Neuro Technology B.V., Enschede, The Netherlands), Brainsight<sup>TM</sup> 2 (Rogue Research Inc., Montreal Quebec, Canada) or NBS System